

# Title An empirical analysis of the dynamics of both individual galaxies and gravitational lensing in galaxy clusters without dark matter

G. Pascoli

Email: pascoli@u-picardie.fr

Faculté des sciences

Département de physique

Université de Picardie Jules Verne (UPJV)

33 Rue Saint Leu, Amiens, France

## Abstract

The existence of the flat rotation curves of galaxies is still perplexing. The dark matter paradigm was proposed long ago to solve this conundrum; however, this proposal is still under debate. In this paper, we search for universal relationships solely involving the baryonic density that incorporate both galactic dynamics and gravitational lensing in galaxy clusters without requiring dark matter. If this type of formula exists, we show that it is possible that it can clearly indicate that dark matter is either perfectly tailored to baryonic matter or, from a more radical point of view, even perhaps useless. If the latter situation is true, then we must give greater visibility to models such as modified inertia (MOND) or even modified gravity (MOG).

**Keywords:** galaxy, galactic rotation, galaxy cluster, dark matter

## 1 Introduction

Many astrophysical observations seem to suggest the existence of a massive and non-baryonic component of the universe called dark matter (DM) (Roszkowski et al., 2018). In the domain of galaxies, the DM paradigm appears very flexible with two adaptable parameters per galaxy, with  $2n$  parameters for  $n$  galaxies. In addition, various types of theoretical DM profiles have been proposed (Bertone, 2010). This high flexibility represents a great advantage compared to other models, such as modified Newtonian dynamics (MOND), which uses one universal parameter (Milgrom, 1983). However, it is also its weakness because it makes the model firmly non-predictive.

Another very perplexing aspect of DM is its intrinsic nature. What is the composition of the DM that supposedly composes approximately 85% of the matter in the Universe? Fritz Zwicky first used the term "dark matter" in the 1930s. By studying the so-called Coma galaxy cluster, he concluded that the very large velocities of the galaxies he measured implied that the cluster had much more mass than the visible matter suggested (Zwicky, 1933). Since then—that is, for ninety years—the scientific community has sought a DM particle. However, it seems very difficult to identify particles with elusive properties, especially when the range of masses and the cross sections are unknown quantities. Despite this fact, theorists have envisioned a wide range of weakly interacting massive particles (WIMPs), representing a leading class of candidates. These particles are predicted in many SUSY models and can be observed in the Large Hadron Collider (LHC). Unfortunately, to date, the LHC has found no signs of WIMP DM (Boveia and Doglioni, 2018; Bertone and Tait, 2018). Other terrestrial searches have also been infructuous (Xenon Collaboration, 2018). On the opposite side in the astrophysical domain, it was proposed that gamma-ray signals could act as DM tracers. However, observations with the Fermi Gamma-Ray Space Telescope in the Small Magellanic Cloud have led to a stringent limit on the DM annihilation cross section (Caputo et al, 2016). A promising path seems to

be comparison of the gamma-ray data coming from the Fermi Large Area Telescope (LAT) and the gravitational lensing data from the Dark Energy Survey (DES) (Ammazzalorso et al, 2020). These researchers found a significant cross correlation between the positions of gravitational lenses, which are thought to trace DM, and those of gamma-ray photons, which are potentially emitted when DM self-destructs. Unfortunately, the statistical analysis of the data remains inconclusive because the cross correlation predominantly comes from blazars. The possibility that these data arise in some small part from DM remains an open question.

Apart from WIMPs as potential candidates, a few researchers have attempted to explain the phenomenon of DM with the introduction of a gas composed of very hypothetical particles of negative mass that could pervade the Universe (Farnes, 2018). However, this proposal provides a worse solution than DM with WIMPs. One reason is that the long-term stability of a disk of positive matter (a galaxy) placed in a halo of negative masses is questionable. A stronger second reason is that with the creation of real particles with negative masses, the vacuum could decay into a lower-energy state so that the vacuum would be unstable. Other reasons to dismiss this bold idea of negative masses are exposed in (Socas-Navarro, 2019).

Ultimately, we can say that the direct proof of the existence of DM or very other exotic particles is rather thin. Other realistic theories that strongly challenge the DM paradigm are MOND (Milgrom, 1983, 2018, 2020; McGaugh, 2015, 2021) and modified gravity or MOG (Moffat, 2008). In contrast to the DM paradigm, whose predictive power is very limited due to its extreme flexibility, both MOND and MOG include only a very small number of parameters. We know that the predictive power of a theory considerably increases when the number of parameters strongly decreases. For instance, MOND with one universal parameter is capable of accurately predicting the shape of the rotation curves in advance of the very-low-density galaxies, while this type of prediction is not possible in the framework of the DM paradigm (McGaugh, 2020).

Finally, we can add a remark on a semantic point of view suggested by McGaugh (2015): “The need for dark matter is often referred to as the *missing mass problem*. This terminology prejudices the answer. More appropriately, the proper terminology should be the acceleration Discrepancy”. It is from this perspective that we conduct our research.

More recently, we have proposed a phenomenological approach, the  $\kappa$  model, with a minimal number of ingredients. From this perspective, we aim to describe the phenomena starting solely from observational data (Pascoli, 2022). Strictly speaking, the  $\kappa$  model is not a theory as can be MOND or MOG. The  $\kappa$  model is based on an empirical relationship, as simple as possible, built on the sole knowledge of the observable quantity, i.e., the baryonic density. At a later stage, a theory may be built. This methodology appears natural for historical reasons. We find notable examples in the history of science: the Kepler laws preceded Newtonian mechanics, and the Rydberg formula preceded quantum mechanics. In contrast, whenever an “additional” ingredient appearing from nowhere has been proposed to explain an experiment or an observation (phlogiston, the aether, the Vulcan planet, etc.), a few decades later, the scholarly community realized its uselessness. This is also possibly the fate expected for DM.

In the present paper, we define the baryonic data, essentially the surface density deduced from the measurement of the luminosity of galaxies, as intrinsic parameters. On the other hand, the DM parameters are defined as extraneous parameters. Is it possible to obtain an agreement between the prediction of a phenomenological model based on the observational data and galactic dynamics by using solely a set of intrinsic parameters, all extraneous parameters, especially DM, being excluded from the list? This proposal is supported by the  $\kappa$  model. The basis relationship links the mean density measured by the terrestrial observer to an intrinsic parameter called  $\kappa$  (Pascoli, 2022). This intrinsic parameter acts as a simple factor for both the inertia term and the active mass or the gravitational constant  $G$  in the dynamics equation. Let us specify that  $\kappa$  is then a calculable quantity directly derived from the baryonic density and not an ad hoc parameter, as in the case of DM.

The  $\kappa$  model hypothesizes that for an observer at a given place (for instance the Earth) the lengths and velocities, associated with any object, located at a very large distance, must be multiplied by a factor  $\kappa$ . This factor is strictly positive-definite. At the Sun position in the Milky Way, i.e., in the solar system,  $\kappa$  is by convention taken equal to unity. Then the final result is that in the dynamics equation, the inertia term is multiplied by  $\kappa$ , mimicking a MOND effect. On the other hand, the gravitational constant  $G$ , or the active mass  $M$ , is multiplied by the inverse factor  $\frac{1}{\kappa}$ , (mimicking an MOG effect) (Pascoli and Pernas, 2020; Pascoli, 2022). However, by contrast to other proposed models or theories, in the  $\kappa$  model, these effects are assumed to be only apparent. In reality, the equations (Newton or Einstein) and the physical constants, when locally considered, are left unchanged, any observer  $O$  being free to locally choose  $\kappa_0 = 1$ . For a terrestrial observer, labelled  $\odot$ , looking at a distribution of matter with a maximum  $\rho_c$ , for instance, a galaxy, the factor  $\kappa$  is ultimately linked to the baryonic mean density  $\rho$  by the following logarithmic functional:

$$\frac{\kappa_c}{\kappa} = 1 + \text{Ln}\left(\frac{\rho_c}{\rho}\right) \quad (1)$$

The mean densities  $\rho$ ,  $\rho_c$  are estimated by the observer  $\odot$ . This relationship is also accompanied by

$$\begin{aligned} \rho_c > \rho_{\odot} \quad \kappa_c &= 1 + \text{Ln}\left(\frac{\rho_c}{\rho_{\odot}}\right) \\ \rho_{\odot} > \rho_c \quad \frac{1}{\kappa_c} &= 1 + \text{Ln}\left(\frac{\rho_{\odot}}{\rho_c}\right) \end{aligned} \quad (2)$$

We can choose by convention  $\kappa_{\odot} = 1$ , which is the value taken by  $\kappa$  at the Sun position in the Milky Way. Note that relations (1) and (2) are empirical laws and must be simply admitted in the  $\kappa$  model and are not derived from it. Thus, other different forms of this type of logarithmic relation can still be suggested under the set of physical conditions, for instance, the range of mean densities or if the matter is either concentrated in compact objects, i.e., stars, or composed of a gaseous bulk. At this stage, we cannot resolve this point. From a practical of view, the formula is expressed as a function of the baryonic surface density  $\Sigma$  (observable and measured) and the thickness  $\delta$  along the line of sight (undetermined, but adjustable), i.e.,

$$\frac{\kappa_c}{\kappa} = 1 + \text{Ln}\left(\frac{\Sigma_c \delta}{\Sigma \delta_c}\right) \quad (3)$$

A supplementary ambiguity is that the thickness can be a function of the radial distance  $r$  in the galaxy. In the present paper, all the fits of the rotation curves are made assuming  $\delta = \text{constant}$  and for the inclination  $i = \text{constant}$  along a galactic radius. The results supplied are thus given at a first-order approximation level, and the rotation curves, which are provided here, are mean curves. Then, a more accurate fit would be obtained by taking into account the variations in  $\delta$  in Eq. (3). Thus, the great advantage of the  $\kappa$  model is that it can be refined with an increased precision for the rotation curves starting from a universal relationship. Unfortunately, the observational resources are limited for both the thickness and the inclination, and we consider this refinement premature at the moment. On the other hand, we do not exclude the suggestion that some amount of unseen baryonic matter very likely exists, for instance, in the form of rogue planets, neutron stars or stellar black holes. A pervasive gas composed of sterile neutrinos can also be invoked (Boyarsky et al, 2019). These ingredients, for which the percentage is unknown, are not taken into account in the present paper but contribute to increasing the baryonic surface density.

Along this path, the case of various spiral galaxies is examined, and we eventually apply the  $\kappa$  model to the Bullet Cluster problem.

## 2 Rotation curves of the galaxies

We begin first with a galaxy composed of a unique discoidal structure and then examine galaxies composed of multiple structures.

### 2.1 NGC 1560

The rotation curve of the low-density galaxy NGC 1560 has already been analysed in the framework of the  $\kappa$  model (Pascoli, 2022). However, this analysis was very succinct, starting from the Newtonian curve supplied by Famaey and McGaugh (Famaey and McGaugh, 2012). Here, we re-examine the question to produce a mean rotation curve without the fluctuations but in a more self-consistent way. The surface density is displayed in Fig. 1. This type of galaxy is idealized as a simple disc. A fit of the surface density can be made with the unique exponential curve

$$\Sigma = \Sigma_{cd} \exp\left(-\frac{r}{r_d}\right) \quad (4)$$

with  $\Sigma_{cd} = 32 M_\odot pc^{-2}$  and  $r_d = 3 kpc$ . The rotation curve for a thin exponential disk is usually expressed by modified Bessel functions (Binney and Tremaine, 1987):

$$v^2(r) = 4\pi G \Sigma_{cd} r_d \left(\frac{r}{2r_d}\right)^2 \left[ I_1\left(\frac{r}{2r_d}\right) K_1\left(\frac{r}{2r_d}\right) - I_0\left(\frac{r}{2r_d}\right) K_0\left(\frac{r}{2r_d}\right) \right] \quad (5)$$

Following the procedure admitted in the  $\kappa$  model (Pascoli, 2022), the velocity, which is measured by spectroscopy, is then given by

$$v_{meas}(r) = p_c^{0.5} \left[ 1 + \text{Ln}\left(\frac{\Sigma_c \delta}{\Sigma \delta_c}\right) \right]^{0.5} v(r) \quad (6)$$

where the factor  $p_c = \frac{1}{\kappa_c}$ . This coefficient is calculated using (2) with the reference  $\Sigma_\odot = 70 M_\odot pc^{-2}$  and  $\delta_\odot = 500 pc$ . To simplify, we chose  $\delta = \delta_c = \delta_\odot$ . Thus, for NGC 1560,  $p_c = 1.78$ . We emphasize that no extraneous parameters are used in the fitting process.

Fig. 2 shows that the  $\kappa$  model produces a mean velocity curve very similar to that of MOND. This result strongly suggests that for NGC 1560, the baryonic distribution alone is sufficient to accurately predict the observed velocity curve, removing the need for DM. The LSB galaxies are in the low-density regime, and following the  $\kappa$  model, the magnification effect of the velocities is then reinforced. Note that the same circumstances arise with MOND because the LSB galaxies are in the low-acceleration regime. Therefore, it is not surprising that both MOND and the  $\kappa$  model provide very similar galactic rotation curves.

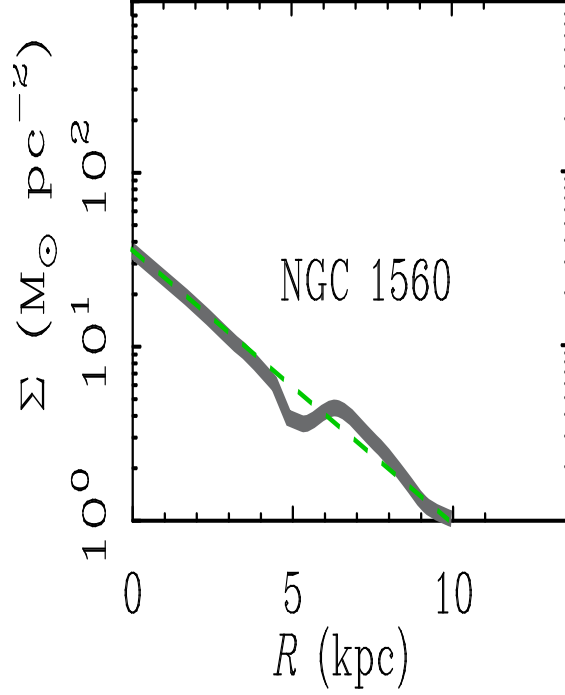


Fig. 1 NGC 1560. The surface density profile is taken from Famaey and Mc Gaugh (2012). The green dashed line is the theoretical fit.

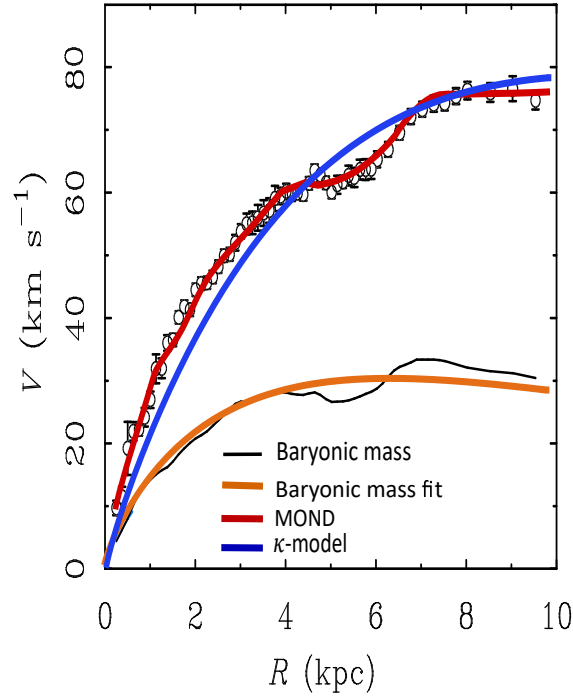


Fig. 2 NGC 1560. Rotation velocity curves.

Note that analytic approximations starting from an exponential disc for the density are no longer valuable to reproduce the fine details (fluctuations) overlaid on the rotation curve. To move forward, we must necessarily take into account the inhomogeneities of the mass distribution. The method is then used to solve a Poisson equation to determine the gravitational potential that corresponds to the observed baryonic mass distribution. Nevertheless, to go beyond the first level of approximation, which directly leads to a mean rotation curve, we need to reach the thickness  $\delta$  along the line of sight (Eq. 3). Knowing the surface density  $\Sigma$  alone is not

sufficient in the  $\kappa$ -model framework. Additionally, the inclination of the galaxy can also vary as a function of the radius  $r$ . These intermixed degeneracies are difficult to remove. Whereas the mean curve is easily reproduced by different theories (DM, MOG or MOND) or within the  $\kappa$  model framework, a total interpretation of the rotation curve of a galaxy with its fluctuations remains ambiguous. This is true for a galaxy such as NGC 1560, which can be valuably fitted with one exponential disc but even more so for complex objects, as we now show.

## 2.2 Dwarf disc galaxies

When the surface density cannot be fitted by a unique exponential profile, the analysis is more complicated. Karukes and Salucci (2017) studied a large sample of dwarf disc galaxies located in the local volume. Those authors showed that a fit of the surface density for these galaxies can be made with a sum of two exponential (stars  $s$  and gas  $g$ ) profiles

$$\Sigma(r) = \frac{M_s}{2\pi r_s^2} \exp\left(-\frac{r}{r_s}\right) + \frac{M_g}{2\pi(3r_s)^2} \exp\left(-\frac{r}{3r_s}\right) \quad (7)$$

Normalizing this relationship immediately gives

$$\sigma(x) = \sigma_s \left[ \exp(-x) + \frac{\alpha}{9} \exp\left(-\frac{x}{3}\right) \right] \quad (8)$$

with two free intrinsic parameters  $\sigma_s = \frac{\Sigma_s}{\Sigma_\odot}$  and  $\alpha = \frac{M_g}{M_s}$  and  $x = \frac{r}{r_s}$ . Fig. 7 of Kekures and Salucci (2017) is reproduced in Fig. 3. The Newtonian curves for the stars (red line) and gas (blue line) correspond to  $\sigma_s = 0.11$  and  $\alpha = 0.62$ . The  $\kappa$ -model profile, superimposed in green, is in practice confounded with the various DM profiles. The  $\kappa$  model gives the same mean rotation curve as the DM paradigm but without extraneous parameters. One conclusion is clear: at least for the dwarf disc galaxies in the local volume, the baryonic contribution is sufficient to explain the rotation curves. Thus, the introduction of DM may be superfluous. We can also take the point of view that the DM mimics an unknown emergent property of the baryonic matter itself at a cosmic macroscale level  $\gtrsim 1\text{kpc}$ . Once again, these considerations give credence to simple models such as MOND and the  $\kappa$  model.

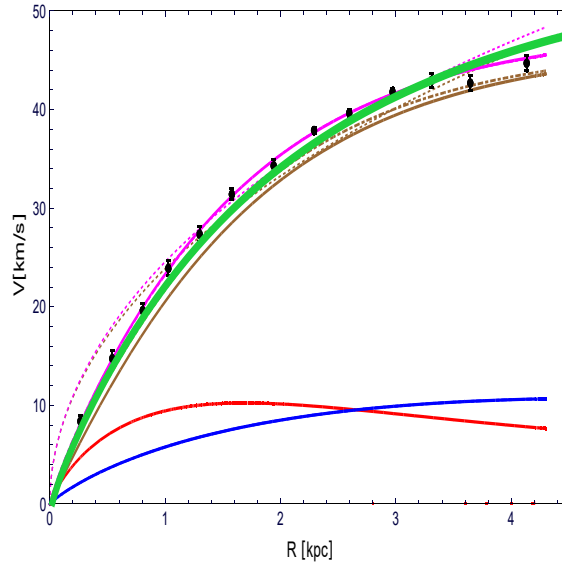


Fig. 3 Synthetic rotation curve for dwarf galaxies (filled circles) and a set of the theoretical curves (red line: stars; blue line: gas; brown line: halo; pink line: the sum of all components) in the case of three DM profiles: the Burkert DM profile (solid line), NFW profile (dotted line) and DC14 profile (dotted-dashed line), from Kekures and Salucci (2017). The  $\kappa$ -model profile is superimposed in green.

### 2.3 NGC 6946

NGC 6946 is composed of multiple structures: a small bulge  $b$ , a stellar disc  $d1$  and a gaseous disc  $d2$  (Fig. 3). The bulge can be modelled by a de Vaucouleurs-type profile (Binney and Tremaine, 1998)

$$\Sigma_{bulge}(r) = \Sigma_{cb} \exp \left[ -8 \left( \frac{r}{r_b} \right)^{\frac{1}{4}} \right] \quad (9)$$

where  $\Sigma_{cb} = 6 \cdot 10^4 \text{ } M_{\odot} \text{ pc}^{-2}$ , and  $r_b = 1 \text{ kpc}$ . The volume mass density for the bulge is then calculated by the well-known formula

$$\rho(r) = \frac{1}{\pi} \int_r^{\infty} dx \frac{d\Sigma_b}{dx} \frac{1}{\sqrt{x^2 - r^2}} \quad (10)$$

and the mass inside the radius  $r$ :  $M(r) = 4\pi \int_0^r dr' r'^2 \rho(r')$ . This leads to a circular velocity of

$$v_b(r) = \sqrt{\frac{G M(r)}{r}} \quad (11)$$

where  $G$  is the gravitational constant.

Each of the discoidal components is modelled with a Gaussian profile as

$$\Sigma_{disc}(r) = \Sigma_{cd} \exp \left[ -\left( \frac{r}{r_d} \right)^2 \right] \quad (12)$$

with ( $\Sigma_{cd1} = 600 \text{ } M_{\odot} \text{ pc}^{-2}$ ,  $r_{d1} = 3 \text{ kpc}$ ) and ( $\Sigma_{cd2} = 10 \text{ } M_{\odot} \text{ pc}^{-2}$ ,  $r_{d2} = 8 \text{ kpc}$ ) (Fig. 4). The stellar and gaseous distributions of matter are then separately treated. We affect the magnification factors  $p_s = \frac{1}{\kappa_s}$  to  $\Sigma_{bulge}(r) + \Sigma_{disc1}(r)$  and  $p_{d2} = \frac{1}{\kappa_{d2}}$  to  $\Sigma_{disc2}(r)$ . These coefficients are calculated from the observational data of  $\Sigma_{cb}$ ,  $\Sigma_{cd1}$  and  $\Sigma_{cd2}$ . Numerically, we find  $p_s = 0.129$  from  $\Sigma_{cb} + \Sigma_{cd1}$  and  $p_g = 2.94$  from  $\Sigma_{cd2}$ . Ultimately, the rotation velocity must be multiplied by the global factor  $\left\{ 1 + \text{Ln} \left[ \frac{\Sigma_{cb}/\delta_{cb} + \Sigma_{cd1}/\delta_{cd1} + \Sigma_{cd2}/\delta_{cd2}}{\Sigma_{bulge}(r)/\delta_{cb} + \Sigma_{disc1}(r)/\delta_{cd1} + \Sigma_{disc2}(r)/\delta_{cd2}} \right] \right\}^{0.5}$ .

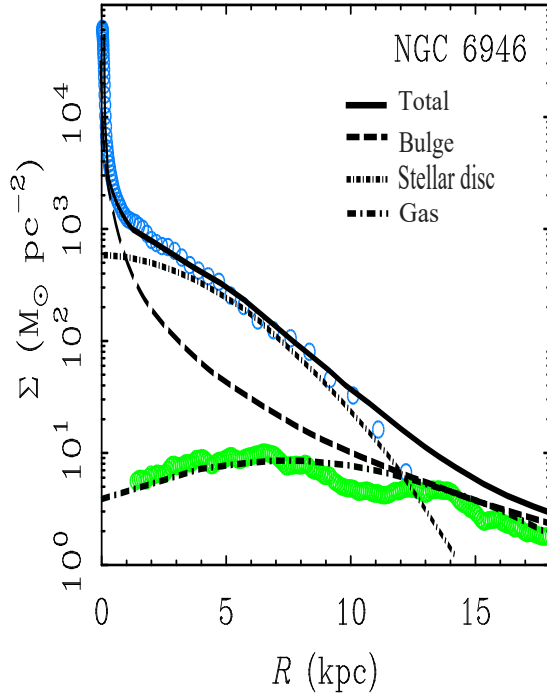


Fig. 4 NGC 6946: Observational surface density profile taken from Famaey and Mc Gaugh (2012) accompanied with the model.

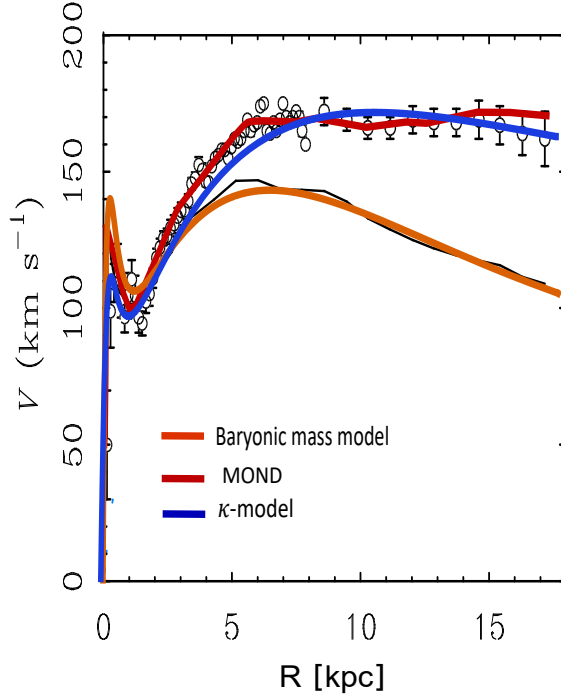


Fig. 5 Rotation curves for *NGC*6946.

Once again, we see good agreement in the figure between MOND and the  $\kappa$  model, together with the observational rotation curve.

## 2.4 M33

M33 is a low luminosity spiral galaxy in the Local Group. Its large angular extent and well-determined distance make it ideal for a detailed study of the radial distribution of matter (Corbelli, 2003). The surface density model adopted here is composed of a stellar disc with an exponential fit  $\Sigma_s(r)$  ( $\Sigma_{cs} = 692 M_\odot pc^{-2}$ ,  $r_{ds} = 1.1 kpc$ ) and a gaseous disc with a Gaussian fit  $\Sigma_g(r)$  ( $\Sigma_{cg} = 15 M_\odot pc^{-2}$ ,  $r_{dg} = 7.6 kpc$ ) (Fig. 6). The velocity is usually multiplied by the magnification factor  $\left\{1 + \ln \left[ \frac{\Sigma_s/\delta_s + \Sigma_g/\delta_g}{\Sigma_s(r)/\delta_s + \Sigma_g(r)/\delta_g} \right] \right\}^{0.5}$ . A good fit, comparable to MOND (Fig. 7), is obtained for  $\delta_g = \delta_s = \delta_\odot$  with the inclination of  $54^\circ$  chosen by Corbelli (2003). However, M33 appears clearly distorted, and the inclination angle of M33 very likely varies in steps with the radial distance  $r$ , as is conspicuous on the observational curve (Fig. 7). Unfortunately, this parameter is difficult to estimate from observations. Once again, the  $\kappa$  model can give a more exact fit by adopting a variable inclination from  $60^\circ$  at 5 kpc to  $48^\circ$  at 15 kpc. Potentially, the  $\kappa$  model can predict the variations in both the inclination and the thickness along the line of sight. This statement is in turn a criterion of falsifiability of the  $\kappa$  model.



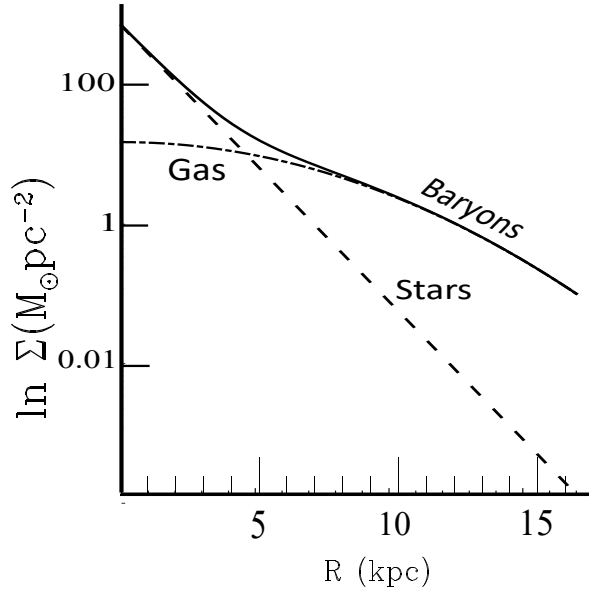


Figure 6 The observational surface density profile (continuous line) is reproduced from Fig. 7 of Corbelli (2003) accompanied by the model described above.

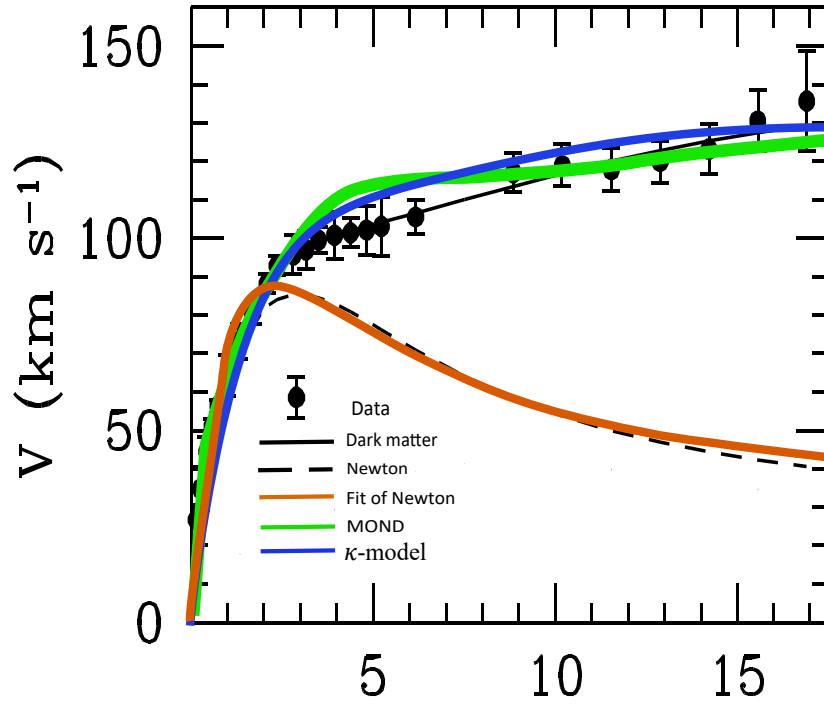


Fig. 7 M33: Rotation curve decompositions

## 2.5 Malin 1

The surface density model adopted here is composed of a thick stellar disc with an exponential profile  $\Sigma_s(r)$  ( $\Sigma_{cs} = 6 \cdot 10^3 M_\odot pc^{-2}$ ,  $r_{ds} = 2 kpc$ ) and a very extended thin gaseous disc with an exponential profile  $\Sigma_g(r)$  ( $\Sigma_{cg} = 4 M_\odot pc^{-2}$ ,  $r_{dg} = 30 kpc$ ) (Fig. 8). With these values, the mass of Malin 1 is on the order of  $1.7 \cdot 10^{11} M_\odot$ . Then, a good fit, similar to the predictions of DM or MOND, is obtained for  $\delta_g = \delta_s = \delta_\odot$  but with a global change in the inclination angle from  $i = 38^\circ$  to  $i = 34^\circ$ . However, because the results vary with thickness in the  $\kappa$  model, a very similar fit is obtained with  $2\delta_g = \delta_s = \delta_\odot$  at constant  $\Sigma$  without a change in the inclination  $i = 38^\circ$ . The rotation curves are displayed in Fig. 9. The DM and the  $\kappa$ -model profiles are

very similar. The MOND profile appears slightly less consistent in the outer regions than the two other profiles, but with a change in the inclination angle in the outer parts of only  $6^\circ$  from  $i = 38^\circ$  to  $i = 32^\circ$ , which cannot be ruled out. According to Lelli et al (2010), MOND is better than both the DM model and the  $\kappa$  model. Thus, the issue is not clearly resolved owing to the uncertainty in the inclination in the outer region. In any case, both the thickness  $\delta$  and the inclinations  $i$  of the discs are variable quantities, which prevents full exploitation of the observational data. Conversely, the  $\kappa$  model could supply predictive and falsifiable information on the mean thickness, but a fuller and more accurate set of observational points would be needed.

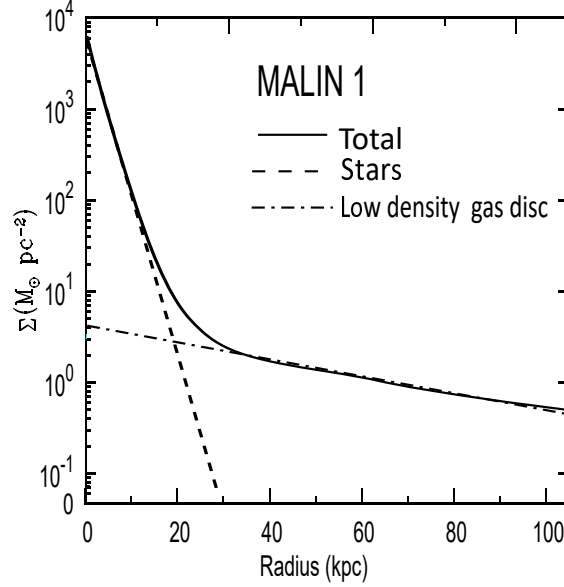


Fig. 8 Observational surface density for Malin1 along a continuous line (from Lelli et al., 2010) and the model.

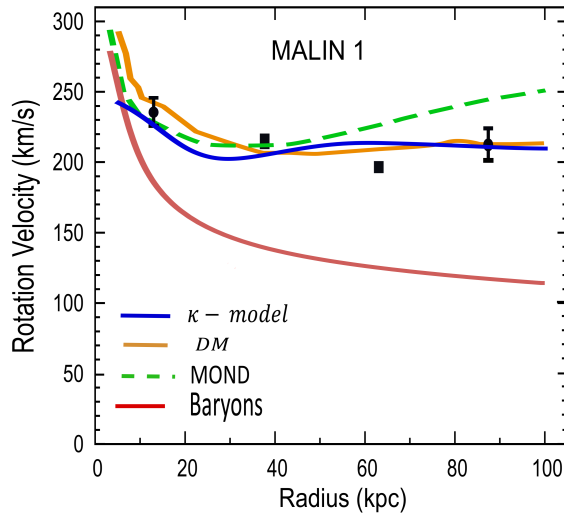


Fig. 9 Malin1 Rotation curve decompositions. Dots with bar errors show the observed rotation curve (from Lelli et al, 2010). The  $\kappa$ -model curve appears in blue.

## 2.6 NGC 7589

The surface density profile is assumed to be decomposed into three parts: a thick disc with an exponential distribution  $\Sigma_s(r)$  ( $\Sigma_{cs} = 3 \cdot 10^3 M_\odot pc^{-2}$ ,  $r_{ds} = 1 kpc$ ), a thin HSB disc  $\Sigma_{HSB}(r)$  ( $\Sigma_{cHSB} = 400 M_\odot pc^{-2}$ ,  $r_{dHSB} = 5.5 kpc$ ) and a thin LSB disc ( $\Sigma_{cLSB} = 10 M_\odot pc^{-2}$ ,  $r_{dLSB} = 15 kpc$ ) (Fig. 10). A good fit for the velocity curve is obtained with an inclination of  $45^\circ$ . The latter value sensibly differs from that given by Lelli et al. (2010), with  $i = 58^\circ$ . The mean rotation curves are displayed in Fig. 11. Another similar solution is still to take  $3\delta_{LSB} = 3\delta_{HSB} = \delta_s = \delta_\odot$  at constant  $\Sigma$ , while now maintaining the inclination suggested by those authors. A mixture of intermediary solutions is clearly possible by exploiting both the inclination and the thickness. *NGC 7589* provides a good example indicating that discrimination between different models can be challenging owing to the indeterminacy impacting these parameters when exploiting the observational material.

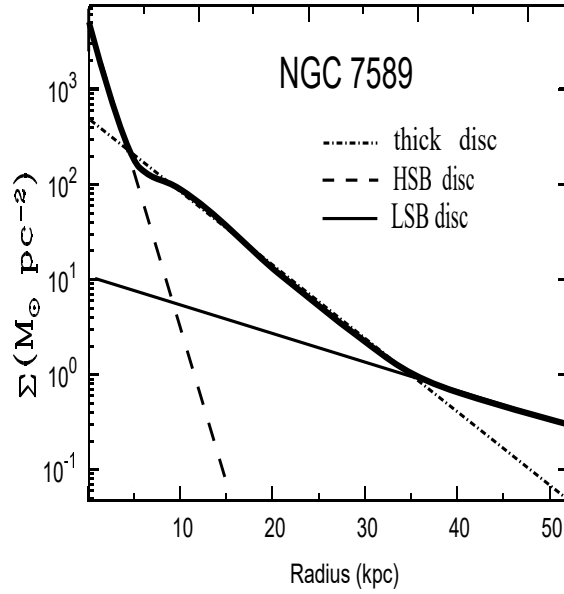


Fig. 10 NGC 7589: Observational surface density along a thick continuous line (from Lelli et al., 2010) and the model.

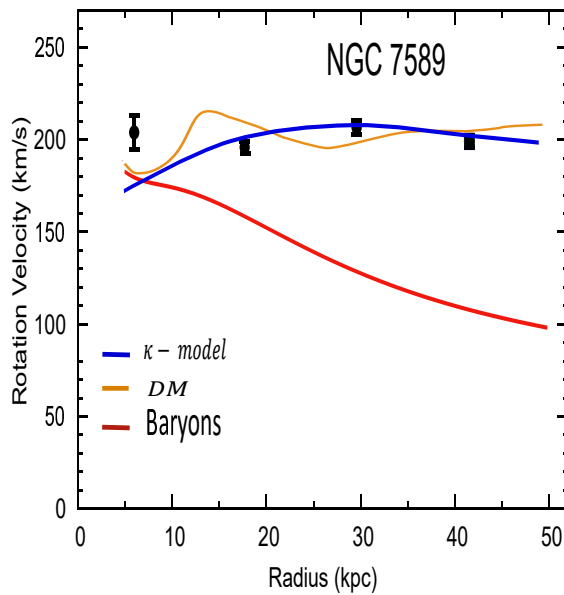


Fig. 11 NGC 7589: Rotation curve decompositions. Dots with error bars show the observed rotation curve (from Lelli et al, 2010). The  $\kappa$ -model curve appears in blue.

## 2.7 M31

*M31* (the Andromeda galaxy) is a near-twin of the Milky Way. Unlike the Milky Way seen from the inside, *M31* is seen from the outside, and both the morphology and The velocity field are much easier to determine.

The surface density is assumed to be composed of three parts: a spherical bulge with a de Vaucouleurs profile ( $\Sigma_{cb} = 4 \cdot 10^3 M_{\odot} pc^{-2}$ ,  $r_b = 1.5 kpc$ ), a stellar disc (*s*) and a gaseous disc (*g*), with the last two represented by an exponential profile ( $\Sigma_{cds} = 4 \cdot 10^2 M_{\odot} pc^{-2}$ ,  $r_b = 5 kpc$ ) and ( $\Sigma_{cdg} = 5 M_{\odot} pc^{-2} r_b = 30 kpc$ ). Note the surface density of the gaseous disc is not uniform but strongly oscillates (Chemin et al, Fig. 16, 2009) and its representation by an exponential profile is necessarily very crude; nevertheless, this simple procedure appears justified by obtaining the mean rotation curve.

Integrating the distributions of matter gives a bulge mass of  $2.5 \cdot 10^{10} M_{\odot}$ , a stellar disc mass of  $6.2 \cdot 10^{10} M_{\odot}$  and a gas disc mass of  $1.7 \cdot 10^{10} M_{\odot}$ , in good agreement with the observational data (Chemin et al, 2009). The mean rotation curve produced by the  $\kappa$  model is displayed in Fig. 12 (caption inserted in the box) together with a set of data given by Chemin et al. Once again, the  $\kappa$ -model and DM profiles are similar. As already ascertained by the latter authors, the peculiar shape of the rotation curve is not readily reproduced by mass distribution models. The central velocity dip cannot be modelled by any fits. Chemin et al. have also shown that between  $r = 6 kpc$  and  $r = 27 kpc$ , a mean inclination of  $(74.3 \pm 1.1^{\circ})$  is derived for the gas disc. A prominent gas warp is detected inside  $r = 6 kpc$ , where the disc appears less inclined, while another external warp detected beyond  $r = 27 kpc$  makes the disc more or less inclined. Two ring-like structures are also observed around  $r = 2.5 kpc$  and  $r = 4.7 - 5.7 kpc$ . A wealth of other details can also be identified. It is very difficult to consider all these peculiarities. The same conclusion applies to the  $\kappa$  model, given that the method we have used automatically leads to a mean rotation curve. Chemin et al. also derived from their results that the dynamical enclosed mass extrapolated at  $r = 159 kpc$  is  $M_{Dyn} \sim 10^{12} M_{\odot}$ , leading to a dark-to-baryonic mass ratio of  $\sim 10$ . For this extrapolated distance, the  $\kappa$  model predicts a very similar magnification factor for the mass,  $\sim 9$ , but without the halo of DM.

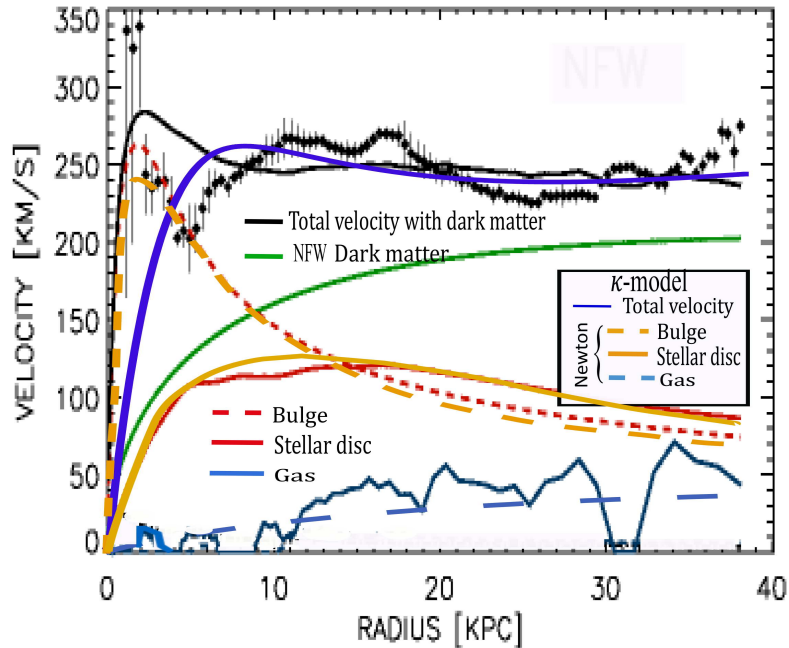


Fig. 12 *M31*: Rotation curve decompositions

We can conclude that starting from mean surface density profiles, the  $\kappa$  model produces adequate mean velocity curves of galaxies, but with the fluctuations smoothed. These fluctuations overlying the observational velocity curves are not accurately taken into account by the  $\kappa$  model at the first level of approximation, nor by the DM paradigm at the same level of approximation. These fluctuations are very likely linked to heterogeneities in the repartition of masses and to variations as functions of the radius  $r$  of both the inclination and the thickness along the line of sight. In any case, these variations are very difficult to estimate, and some ambiguity is inevitable in the interpretation of the results, regardless of the model or theory: DM, MOND, MOG,  $\kappa$  model, . . . . If the variation in both the inclination and the thickness along the line of sight were explicitly considered the  $\kappa$ -model could reproduce the fluctuations seen on the rotation curves, but at the cost of degeneracies. Notably, this is also true for any other model.

### 3 Bullet Cluster

We now apply the  $\kappa$  model to the Bullet Cluster by using the procedure proposed for the individual galaxies. For that, a small set of relations built from an imposed and unique pattern is used. Only baryonic parameters are taken into account. The cluster of galaxies 1E0657-56, or the so-called Bullet Cluster, is one of the hottest, most X-ray-luminous clusters known (Tucker, Tananbaum and Remillard, 1998). Chandra observations by Markevitch et al. (2002) revealed the cluster to be a supersonic merger. The interpretation that prevails today is that the dissipationless DM accompanying the stellar component has bypassed the X-ray-emitting hot plasma region during the collision (Fig. 13). Thus, due to its remarkable morphology, the Bullet Cluster is presumed to be the best known system in which to test the DM paradigm (Clowe et al., 2006). More specifically, the repartition of DM has been indirectly estimated by the combined strong and weak lensing reconstruction method developed by Bradač et al. (2005, 2006). Following this view, the dark matter clump revealed by the strong and weak lensing map is coincident with the collisionless galaxies but lies ahead of the X-ray-collisional gas. Let us note, however, that gravitational lensing observations can also be explained by two theories that do not require DM: MOG (Browstein and Moffat, 2007) and an extension of MOND (Skordis and Złóćnik, 2021).

The issue also deserves analysis in the framework of the  $\kappa$  model. As shown in Fig. 13, the X-ray-emitting hot plasma (in pink), which contains the bulk of the baryonic Matter, is localised in the central region of the cluster, while most of the apparent mass as measured by gravitational lensing, i.e., the stellar component plus DM (in blue), appears on both sides of this bulk.

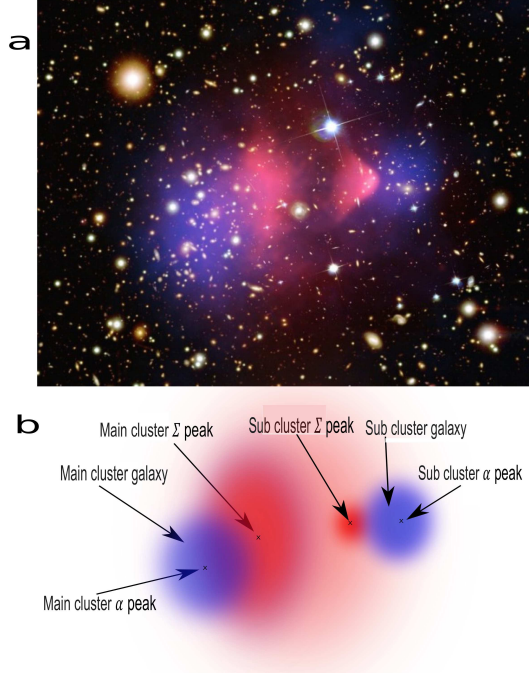


Fig. 13a. Bullet Cluster (from the Chandra X-ray Observatory: 1E 0657-56), b. the model

For the Bullet Cluster, as in the preceding study of the individual galaxies and in accordance with the  $\kappa$  model, only the intrinsic parameters linked to the baryonic matter are taken into account.

The surface density is then modelled by a series of Gaussians as

$$\Sigma(x, y) = \sum_{i=1}^5 \Sigma_i(x, y) = \sum_{i=1}^5 \Sigma_{ci} \exp\left\{-\frac{(x - a_i)^2}{c_i} - \frac{(y - b_i)^2}{d_i}\right\} \quad (13)$$

Each  $\Sigma_i$  is then multiplied by a weighting coefficient introduced to simulate either the presence of DM or, in the case of the  $\kappa$  model, an effect of magnification or even reduction (depending on the location of the observer in a region of either low or high mean density). With this methodology, we fit the profiles of density presented by Browstein and Moffat (2007) in their full analysis of the Bullet Cluster (Browstein and Moffat, Fig. 15a and 15b, 2007). The results are displayed in Fig. 14.

Component	Main cluster	Subcluster
$M_g$	$\Sigma_{cg1} = 0.030, a_{g1} = 0.0, b_{g1} = 0.0, c_{g1} = 3.3, d_{g1} = 6.6$	$\Sigma_{cg} = 0.035, a_g = 0.7, b_g = 0.1, c_g = 0.05, d_{g1} = 0.05$
	$\Sigma_{cg2} = 0.045, a_{g2} = 0.0, b_{g2} = 0.0, c_{g2} = 0.25, d_{g2} = 0.5$	
$M_{gal}$	$\Sigma_{cgal} = 0.02, a_{gal} = -0.4, b_{gal} = -0.2, c_{gal} = 0.06, d_{gal} = 0.06$	$\Sigma_{cgal} = 0.032, a_{gal} = 1.1, b_{gal} = 0.2, c_{gal} = 0.06, d_{gal} = 0.06$
$M_{DM}$	$p_{cg1} = 2, p_{cg2} = 4, p_{cgal} = 7$	$p_{cg} = 2, p_{cgal} = 7$

Table 1 DM model: the surface densities  $\Sigma_{ci}$  are normalized relative to  $\Sigma_0 = 3.1 \cdot 10^3 M_{\odot} pc^{-2}$

In the  $\kappa$  model, each magnification factor  $p_{ci}$  for each Gaussian component is obtained from the

main relationship

$$p_{ci} = 1 + Ln\left(\frac{\Sigma_{\odot}\delta_{ci}}{\Sigma_{ci}\delta_{\odot}}\right) \quad (14)$$

where  $\Sigma_{ci}$  and  $\delta_{ci}$  respectively designate the surface density and the thickness at the maximum of each Gaussian component  $i$  and where  $\Sigma_{\odot} = 70 M_{\odot} pc^{-2}$  and  $\delta_{\odot} = 500 pc$  respectively designate the surface density and the mean thickness taken at the Sun's position in the Milky Way. These factors are relative to the terrestrial observer; observers located elsewhere would obtain different coefficient values. In particular, Table 2 shows that an estimate by the terrestrial observer gives a value on the order of 6. Most notably, this is the same value as for the amplification factor, which is given by Brownstein and Moffat (2007, Fig. 7) for the gravitational constant. The difference is that in the  $\kappa$  model, this factor is calculated, whereas in the MOG framework proposed by these authors, an extraneous parametrization is made that modifies  $G$ . In the  $\kappa$  model, the magnification factor results solely from knowledge of the baryonic density. On the other hand, in the  $\kappa$ -model framework, the gravitational constant  $G$ , locally measured by a very distant observer, is the terrestrial Newtonian gravitational constant measured experimentally on Earth. The relation (14) is valid for the evaluation of the spectroscopic velocities in a galaxy or a galaxy cluster. This factor corresponds to the usual DM effect as it is perceived from the Earth. However, for gravitational lensing, another set of coefficients must be used; let

$$p'_{ci} = 1/(1 + Ln[\frac{\Sigma_{ci}/\delta_i}{\rho_{min}}]) \quad (15)$$

The reason we follow this procedure is that, in the  $\kappa$ -model framework, we must necessarily choose a reference point where the distribution of matter is maximized. For a galaxy, this is its centre, which is common to all the distributions for both gas and stars. For the Bullet Cluster, the situation is different, and there are several maximums. Therefore, to determine the lensing diagram, we necessarily use a common reference for the densities. We choose the most natural basis: the baryonic background volume density,  $\rho_{min} \sim 10^{-25} kg m^{-3}$  (Brownstein and Moffat, 2007). The factors  $p'_{ci}$  are gathered in Table 2.

We must also take into account a global factor at the selected point with coordinates  $(x, y)$ :  $1 + Ln[\frac{\sum_{i=1}^5 \Sigma_i(x, y)/\delta_i}{\rho_{min}}]$ .

The coefficient (15) does not generate a magnification but rather a reduction in the lensing. Indeed, a potential observer living in a very-low-density environment would see an apparent reduction in the lensing and not a magnification. At the same time a significant effect is a displacement of the peaks of the lensing diagram near the centre of each galaxy cluster as due to the factor  $1 + Ln[\frac{\sum_{i=1}^5 \Sigma_i(x, y)/\delta_i}{\rho_{min}}]$ .

Component	Main cluster	Subcluster
$M_g$	$\Sigma_{cg1} = 0.03, a_{g1} = 0.0, b_{g1} =$	
	$0.0, c_{g1} = 3.3, d_{g1} = 6.6$	
	$\delta_{g1} = 2.6, p_{cg1} = 8.6, p'_{cg} = 0.21$	$\Sigma_{cg} = 0.035, a_g = 0.7, b_g = 0.1, c_g =$
	$\Sigma_{cg2} = 0.045, a_{g2} = 0.0, b_{g2} =$	$0.05, d_g = 0.05$
	$0.0, c_{g2} = 0.25, d_{g2} = 0.5$	$\delta_g = 0.22, p_{cg} = 5.9, p'_{cg} = 0.14$
$M_{gal}$	$\delta_{g2} = 0.7, p_{cg2} = 6.9, p'_{cg2} = 0.16$	
	$\Sigma_{cgal} = 0.025, a_{gal} = -0.4, b_{gal} =$	$\Sigma_{cgal} = 0.032, a_{gal} = 1.1, b_{gal} =$
	$-0.2, c_{gal} = 0.06, d_{gal} = 0.06$	$0.2, c_{gal} = 0.06, d_{gal} = 0.06$
	$\delta_{gal} = 0.24, p_{cgal} = 6.4, p'_{cgal} = 0.14$	$\delta_{gal} = 0.24, p_{cgal} = 6.1, p'_{cgal} = 0.14$

Table 2 The  $\kappa$  model: the surface densities  $\Sigma_{ci}$  are normalized relative to  $\Sigma_0 = 3.1 \cdot 10^3 M_{\odot} pc^{-2}$  and the coefficients  $\delta_i$  (the mean thickness along the line of sight) to  $500 kpc$ . The coefficient of normalization for the volume density is  $\rho_0 = 3.6 \cdot 10^{-22} kg m^{-3}$ .

The lensing diagram is reported to the terrestrial observer by multiplying by the constant factor  $p = 1 + Ln(\frac{\Sigma_{\odot}/\delta_{\odot}}{\rho_{min}})$ . The latter factor is a simple multiplicative constant and leaves unchanged the orientation of the deviation vectors of light rays and the position of the peaks in the lensing diagram, but it now produces a global magnification  $\sim 10$  of the lensing. This set of coefficients must be admitted as empirical factors following a similar protocol as for the individual galaxies. Although there is no theoretical justification at this stage for these empirical formulae, the great interest of the approach is that no extraneous parameters linked to hypothetical DM are introduced in the reasoning.

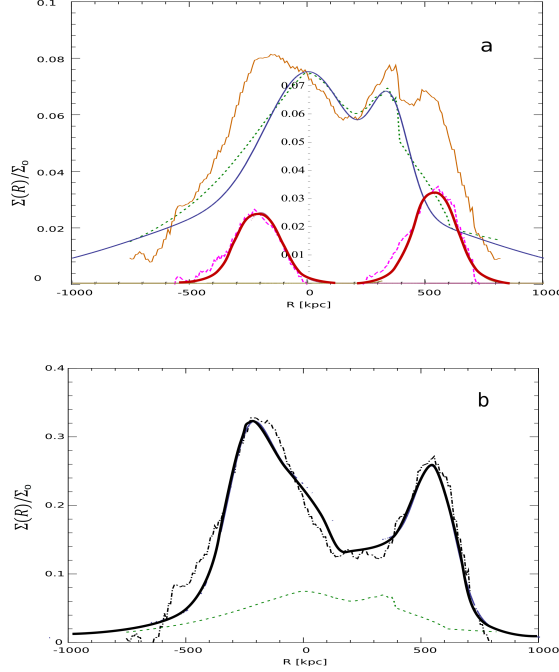


Fig. 14. Bullet Cluster: a. Plots of the scaled surface densities along the line connecting the galaxy cluster peaks. The contribution of galaxies is shown in long-dashed magenta, and the total visible baryonic mass is shown in solid brown. The gas distribution is shown in short-dashed green on plots a and b (from Browstein et Moffat, Fig. 15, 2007). Our fits are shown in red for the galaxies and in blue for the gas. b. The DM contribution is shown in dashed-dotted black (from Browstein et Moffat, Fig. 15, 2007). Our fit from Table 1 is in solid black.

The  $\kappa$  model is based on an empirical relationship and is not a theory by itself. A theory must still be chosen as support, for instance, Newtonian dynamics for the rotation curves of individual galaxies and general relativity for the gravitational bending of light by mass. We know that galaxy clusters can produce noticeable lensing effects. The field equations of general relativity can be linearised if the gravitational field is weak. Then, the deflection angle of a set of masses is simply the vectorial sum of the deflections due to individual lenses. Let  $(x, y)$  be the plane of the sky. The deviation angle  $\alpha$  can be written using the thin lens approximation as (Bartelmann and Schneider, 2001)

$$\alpha(x, y) = \sum_{i=1}^5 \left[ \int_{\text{component } i} dx' dy' \frac{4G}{c^2} \Sigma_i(x', y') \frac{\mathbf{r} - \mathbf{r}'}{|\mathbf{r} - \mathbf{r}'|^2} \right] \quad (16)$$

where  $G$  is the gravitational constant and  $c$  is the speed of light. The  $\kappa$  model does not change the local physics, apart from magnification factors. Thus, in this model, the relation



(16) immediately becomes

$$\alpha(x, y) = p \left\{ 1 + \text{Ln} \left[ \frac{\sum_{i=1}^5 \Sigma_i(x, y) / \delta_i}{\rho_{min}} \right] \right\} \sum_{i=1}^5 p'_{ci} \left[ \int_{\text{component } i} dx' dy' \frac{4G}{c^2} \Sigma_i(x', y') \frac{\mathbf{r} - \mathbf{r}'}{|\mathbf{r} - \mathbf{r}'|^2} \right] \quad (17)$$

In Fig. 15, the results for  $|\alpha(x, y)|$  are displayed for the sole baryonic contribution (Fig. 15a), taking into account the DM component (Fig. 15b) and the  $\kappa$ -model framework (Fig. 15c). Subfigure a shows that in the case of the sole baryonic contribution, as appropriate, the lensing diagram is centred on the bulk of hot gas that is the most massive and dense component in the cluster. On the other hand, the lensing is small. This situation dramatically changes with the introduction of the DM (Fig. 15b) or within the  $\kappa$ -model framework, where in the latter, the density effect is taken into account (Fig. 15c). A bipolar configuration then appears with two poles centred on the galaxies. Comparison of Fig. 15b and 15c indicates that the lensing diagrams are similar.

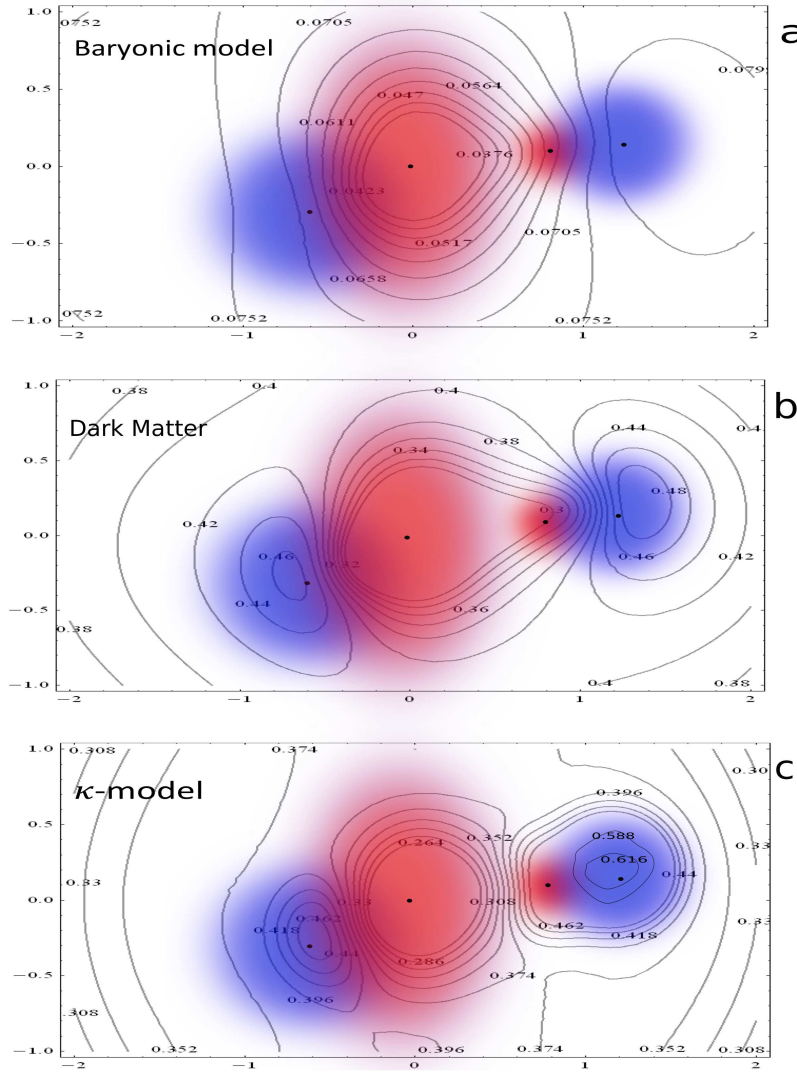


Fig. 15. Bullet Cluster, lensing diagrams: a. baryons, b. DM, and c. the  $\kappa$  model

## 4 Conclusion

We have succeeded in showing that a set of results concerning the dynamics of individual galaxies or gravitational lensing in clusters of galaxies can be fitted with one unique component, i.e., baryonic matter. Thus, rather than invoking exotic particles, a much more efficient path consists of following the historical order in science: Kepler laws preceded Newtonian mechanics, and the Rydberg formula preceded quantum mechanics. In the present context, coming first are empirical relationships built on the sole characteristics of baryonic matter. If this type of relation exists, then a direct link between the baryonic surface densities and the galactic rotation curves is automatically designed. Next, we elaborate a theory supporting and explaining these relationships following, for instance, MOND or one of its more sophisticated extensions. Similarly, even though the procedure adopted in the present paper is based upon the use of very simple “recipes”, this strongly suggests that models such as MOND or the  $\kappa$  model are privileged against other contingencies that introduce extraneous and experimentally undetected particles, such as DM or negative masses. A question, however, remains: why can a model that takes into account solely baryonic data be derived at the first level of approximation (smoothing the fluctuations) with rotation curves similar to those of the DM paradigm, which uses extraneous parameters? This question requires further thought. We can assume that the DM effect represents intrinsic properties of the baryonic matter itself. When the acceleration is very low MOND (Milgrom, 1983) proposed a modification of the inertia term. On the other hand MOG (Moffat, 2008) predicts an increase in the gravitational constant in the long-range domain. The phenomenological  $\kappa$  model (Pascoli, 2022) suggests a renormalization of the dynamics equation with the following consequence: an apparent modification of both inertia and the gravitational constant. Let us also note a promising extension of MOND as developed by Skordis and Złótnik (2021).

On the other hand, the issue is far from being settled at a much higher level of approximation because accurate observational rotation curves and a precise estimate of the surface densities is then needed to discriminate between all the competitors: DM, MOG, MOND or even the  $\kappa$  model. Unfortunately, at present, the observational rotation velocity curves very often vary substantially from one author to another. Another difficulty is the uncertainties in the mass-to-light ratio. This parameter must be very accurately estimated to deduce a valuable surface mass density; otherwise, the quality of a model cannot be evaluated. With the first objective achieved, the next step in the  $\kappa$ -model framework is to go beyond the first level of approximation supplied here. The aim is to build a self-consistent procedure linking the baryonic surface density and the rotation curve for any galaxy by taking into account the heterogeneities and the variation in both thickness and inclination, all without any extraneous parameters.

**Data availability statement:** The author confirms that the data supporting the findings of this study are available within the article and the reference list.

**Conflicts of Interest:** The author declares no conflict of interest.

## 5 References

- Ammazzalorso, S., et al., 2020, Phys. Rev. Lett., 124, 101102
- Bartelmann, M., & Schneider, P., 2001, Physics Reports, 340, 291
- Bertone, G., 2010, Particle Dark Matter: Observations, Models and Searches, Cambridge University Press. p. 762, ISBN 978-0-521-76368-4
- Bertone, G., & Tait, T. M. P., 2018, Nature, 562, 51
- Binney, J., & Merrifield, M., 1998, Galactic Astronomy, Princeton University Press
- Boveia A., & Doglioni, C. , 2018, Annual Review of Nuclear and Particle Science, 68, 429

Boyarsky, A., Drewes, M., Lasserre, T., Mertens, S., Ruchayskiy, O., 2019, Progress in Particle and Nuclear Physics, 104, 1  
 Bradač, M., Schneider, P., Lombardi, M., & Erben, T., 2005, A & A, 436, 39  
 Bradač, M., Clowe, D., Gonzalez, A.H., Marshall, P., Forman, W., Jones, C., Markevitch, M., Scott Randall, S., Schrabback, T., & Zaritsky, D., 2006, ApJ, 652, 937  
 Browstein, J.R., & Moffat, J., 2007, MNRAS, 382, 29  
 Caputo, R., Buckley, M.R., Martin P., Charles, E., Brooks, AM., Drlica-Wagner, A., Gaskins, J., & Wood, M., 2016, Phys. Rev. D **93**, 062004  
 Chemin, L., Carignan, C., & Foster, T., 2009, ApJ, 705, 1395  
 Clowe, D., Bradač, M., Gonzalez, A.H., Markevitch, M., Randall, S.W., Jones, C., & Zaritsky, D., 2006, ApJ, 648, L109  
 Corbelli, E., 2003, MNRAS, 342, 199  
 Corbelli, E., & Salucci, P., 2007, MNRAS, 374, 1051  
 Famaey, B., & McGaugh, S.S., 2012, Living Rev. Relativity, 15, 10  
 Farnes, A., 2018, A & A., 620, A92  
 Karukes, E.V., & P. Salucci, P., 2017, MNRAS, 465, 4703  
 Lelli, F., Fraternali, F. & Sancisi, R. 2010, Astronomy & Astrophysics, 516, A11  
 López-Corredoira, M., & Betancort-Rijo J.E., 2021, ApJ, 909, 137  
 Markevitch, M., Gonzalez, A. H., David, L., Vikhlinin, A., Murray, S., Forman, W., Jones, C., & Tucker, W. 2002, ApJ, 567, L27  
 Mc Gaugh, S., 2015, Canadian Journal of Physics 93, 250  
 Mc Gaugh, S., 2020, Galaxies, 8, 35  
 Milgrom, M., 1983, ApJ, 270, 365  
 Milgrom, M., 2019, arXiv: 1910.04368v3  
 Milgrom, M., 2020, Studies in the History and Philosophy of Modern Physics, 71, 170  
 Moffat, J.W., 2006, J. Cosmol. Astropart. Phys., 2006, 4  
 Moffat, J.W., 2008, Reinventing Gravity, Eds. HarperCollins  
 Pascoli G., & Pernas L., 2020, hal.archives-ouvertes.fr/hal-02530737  
 Pascoli, G., 2022, Astrophys. Space Sci., 367, 121  
 Roszkowski, L., Sessolo, E.M., & Trojanowski, S., 2018, Rep. Prog. Phys., 81, 066201  
 Skordis, C., & Złótnik, T., Phys. Rev. Lett., 127, 161302 (2021)  
 Socas-Navarro, H., 2019, A&A, 626, A5  
 Tucker, W.H., Tananbaum, H., & Remillard, R.A., 1998, ApJ, 496, L5  
 Xenon Collaboration, 2018, Phys. Rev. Letters 121, 111302.  
 Zwicky, F., 1933, Helvetica Physica Acta, 6, 110